A short evaluation of triangulated range from multiple angles-only sites

Zachary Slatton

614 AOC/SSD

Abstract

Range observations are scarce for deep space objects. This scarcity sometimes lowers the accuracy of ephemerides. This is especially true for sparsely tracked angles-only objects, objects with too short fit spans, and objects that are created from angles-only uncorrelated tracks. This paper evaluates the use of triangulated range for objects that have been simultaneously tracked by two or more angles-only sites. Evaluated are the accuracy of the triangulated range and the error growth of ephemerides when triangulated range is included in the differential correction.

1. Introduction

Triangulation is the derivation of the range of an object using two or more sets of angles. It has been used in many fields including the tracking of space objects. Range data helps give a more accurate solution when calculating ephemerides because it refines the size and shape of an orbit when included with angles. Radars are the most common source of range data, but for radar sensors, when an object gets further away from the site the signal to noise ratio (SNR) decreases by a power of four. For optical sensors, the further away an object gets from the site SNR decreases by a power of two. For this reason most of the objects in deep space are tracked by optical sites. Optical sites have a physical limitation in that they cannot measure the range of an object. However, by using more than one optical sensor the range can be calculated with triangulation. Other networks of space trackers have taken advantage of triangulated ranges already.

The concept presented here involves using two Ground Based-Electro-Optical Deep Space Surveillance (GEODSS) telescopes simultaneously tracking the same object and deriving a range from the resulting angles-only observations. Only two regimes will be evaluated, geosynchronous and Molniya, as these are the most populated regimes in deep space. At the geosynchronous belt, there are roughly sixty-six degrees of longitude where simultaneous tracking with two GEODSS sites is possible.

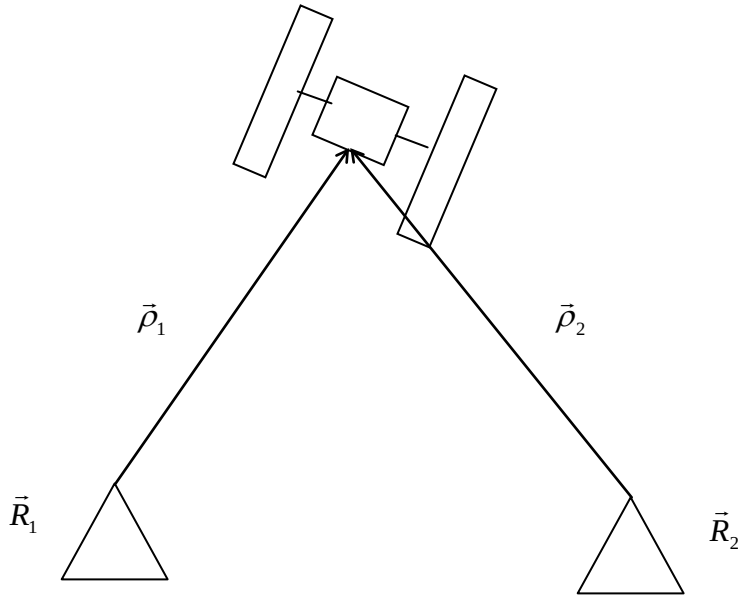

Figure 1: Simultaneous Tracking to Derive Range

2. Triangulation Algorithm

For the position of a satellite:

$$\rho * \hat{\rho} + \vec{R} = \vec{r} \qquad \text{Eq(1)}$$

Where ρ is the range, $\hat{\rho}$ is the pointing vector, $\vec{R}$ is the sensor position in the earth-centered inertial (ECI) coordinate frame, and $\vec{r}$ is the satellite position also in the ECI coordinate frame.

$$\hat{\rho} = \begin{bmatrix} \cos(\delta_t) * \cos(\alpha_t) \\ \cos(\delta_t) * \sin(\alpha_t) \\ \sin(\delta_t) \end{bmatrix} \qquad \text{Eq(2)}$$

Where δ_t is the topocentric declination and α_t is the topocentric right ascension.

If two sensors track the satellite at the same time, the equation can be written as:

$$\rho_1 * \hat{\rho}_1 + \vec{R}_1 = \rho_2 * \hat{\rho}_2 + \vec{R}_2 \qquad \text{Eq(3)}$$

The range can then be solved by the least squares solution of the equation:

$$\begin{bmatrix} \hat{\rho}_1 & -\hat{\rho}_2 \end{bmatrix} * \begin{bmatrix} \rho_1 \\ \rho_2 \end{bmatrix} = \vec{R}_2 - \vec{R}_1 \qquad \text{Eq(4)}$$

If multiple sensors track the satellite at the same time, the equation becomes:

$$\begin{bmatrix} \hat{\rho}_1 & -\hat{\rho}_2 & 0 & . & 0 \\ 0 & \hat{\rho}_2 & -\hat{\rho}_3 & & . \\ . & & . & . & \\ 0 & . & . & \hat{\rho}_{n-1} & -\hat{\rho}_n \end{bmatrix}_{3*(n-1)xn} * \begin{bmatrix} \rho_1 \\ \rho_2 \\ . \\ \rho_n \end{bmatrix}_{nx1} = \begin{bmatrix} \vec{R}_2 - \vec{R}_1 \\ \vec{R}_3 - \vec{R}_2 \\ . \\ \vec{R}_n - \vec{R}_{n-1} \end{bmatrix}_{3*(n-1)x1} \qquad \text{Eq(5)}$$

If right ascension-rate and declination-rate are also provided, a range-rate can also be derived by using the ranges derived previously.

$$\begin{bmatrix} \hat{\rho}_1 & -\hat{\rho}_2 & 0 & . & 0 \\ 0 & \hat{\rho}_2 & -\hat{\rho}_3 & & . \\ . & & . & . & \\ 0 & . & . & \hat{\rho}_{n-1} & -\hat{\rho}_n \end{bmatrix}_{3*(n-1)xn} * \begin{bmatrix} \dot{\rho}_1 \\ \dot{\rho}_2 \\ . \\ \dot{\rho}_n \end{bmatrix}_{nx1} = \begin{bmatrix} \dot{\vec{R}}_2 - \dot{\vec{R}}_1 + \rho_2\dot{\hat{\rho}}_2 - \rho_1\dot{\hat{\rho}}_1 \\ \dot{\vec{R}}_3 - \dot{\vec{R}}_2 + \rho_3\dot{\hat{\rho}}_3 - \rho_2\dot{\hat{\rho}}_2 \\ . \\ \dot{\vec{R}}_n - \dot{\vec{R}}_{n-1} + \rho_n\dot{\hat{\rho}}_n - \rho_{n-1}\dot{\hat{\rho}}_{n-1} \end{bmatrix}_{3*(n-1)x1} \qquad \text{Eq(6)}$$

3. Interpolation of the Angles

An accurate triangulation depends on the observations from the sites to be acquired at the exact same time. Since this is unrealistic a method of interpolating the angles of one site to the time of the observations from the second site has been derived. If a set of observations of one site falls between two sets of observations from the second site, the angles of the second site can be propagated to the time of observations from the first site.

For any two sets of observations from the same site that are taken close together a rate of the pointing vector can be calculated as:

$$\dot{\hat{\rho}} = \frac{\hat{\rho}_2 - \hat{\rho}_1}{t_2 - t_1} \qquad \text{Eq(7)}$$

Where t is the time of the observation and $\dot{\hat{\rho}}$ is the time rate of change of the pointing vector. The new pointing vector can then be calculated at the time of the other site:

$$\rho_T = \hat{\rho}_1 + \dot{\hat{\rho}} * (T - t_1) \qquad \text{Eq(8)}$$

Where ρ_T is the pointing vector interpolated to the time of the other site's observation set.

Also needed, is the position of the second site at the time of the observations of the first site. This accounts for the movement of the sensor due to the Earth's rotation or the change in position if using a mobile sensor. From this point forward the term triangulation will refer to the interpolation before the triangulation as well as the triangulation.

4. Methods of Analysis Using Historical Data

Method 1, shown in figure 2, evaluates the triangulated range. To determine how accurate it is, the range residuals after differential correction (DC) are evaluated. The DC theory being used is SGP4. The element set after the DC is then used to obtain range residuals of the triangulation by using the Astrodynamic Standards' Report Observation Tag and Association Status (ROTAS). On average a good range has a residual of less than 2 kilometers for geosynchronous satellites.

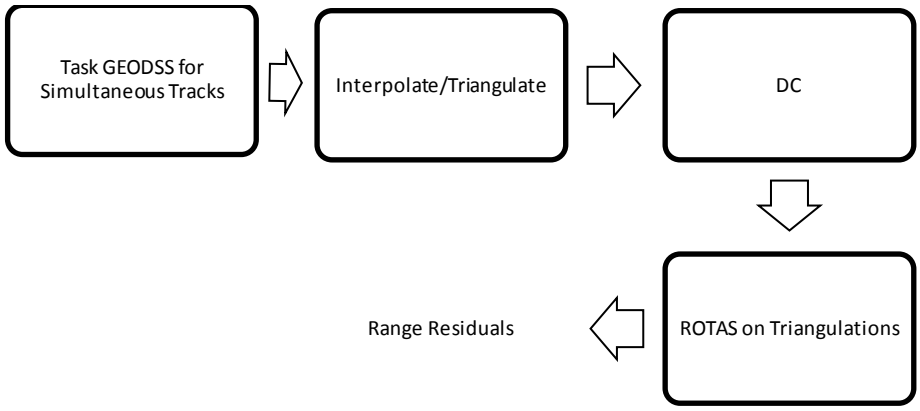

Figure 2: Range Evaluation (Method 1)

Method 2, shown in figure 3, evaluates the difference of error growth when triangulated range was included in the DC and when it was not included. When doing the DC it is important to use the exact same observations except for the inclusion of the new triangulated range. The error was modeled by looking at the residuals of the observations after the epoch of the DC.

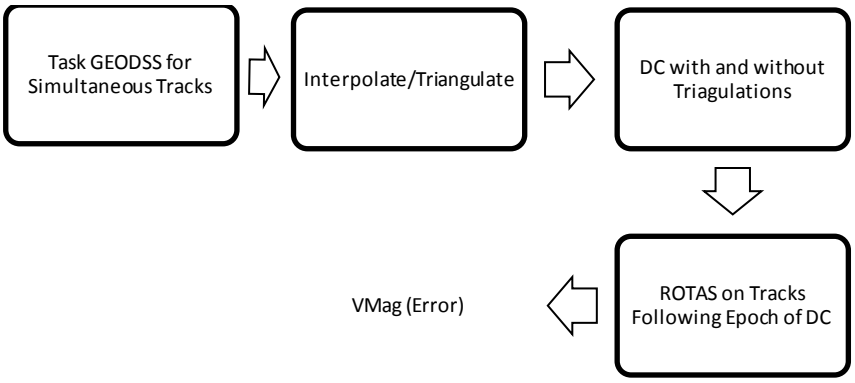

Figure 3: Error Evaluation (Method 2)

Method 3, shown in figure 4, evaluates the error growth of an uncorrelated track (UCT) that was simultaneously tracked by two GEODSS sites. The simultaneous tracking is handled differently. One GEODSS site has to track the object for a few hours, make an element set, and send it to the other site so that they can also track the object. The observations must undergo an initial orbit determination (IODET) before the DC. After the element set is corrected with the triangulation and an analyst satellite is created, the sensor is tasked to obtain another track on the new analyst satellite. The error of the new track is then evaluated.

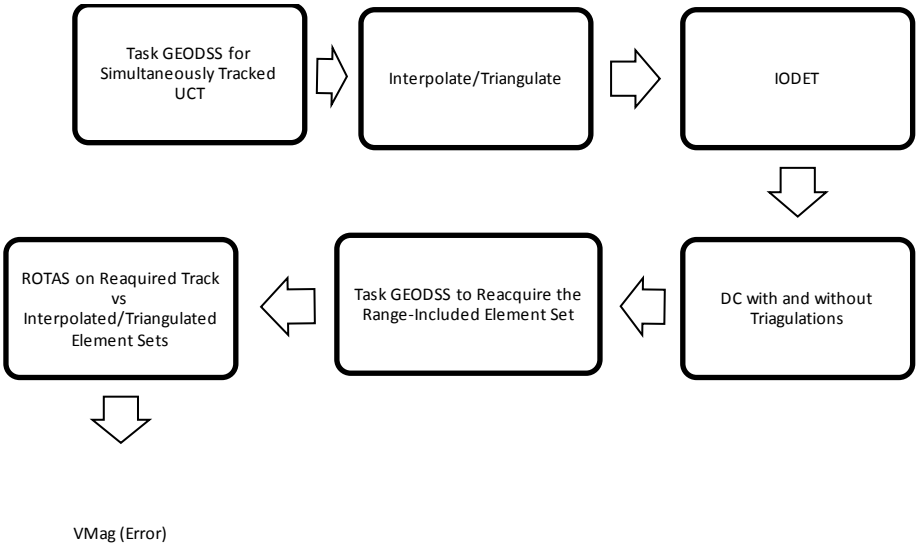

Figure 4: UCT Error Evaluation (Method 3)

5. Results

Table 1 shows the range residuals obtained using Method 1. The objects were randomly selected from a list of objects that were able to be seen by both the Socorro and Maui GEODSS sites. The average range residual of a triangulated observation at geosynchronous orbit is 1.6km, which is a historically accurate value if only a little worse than a mechanical tracker. However, the standard deviation for each track is fairly high which means the triangulated ranges are noisy. The standard deviation for a mechanical tracker is usually less than a tenth of a kilometer. The Molniya orbits are better with an average range residual of 1.1 km which is within the span of range residuals for mechanical trackers seen in Table 2. However, the triangulated ranges still have high standard deviations for each track.

Table 1: Triangulated Range Residuals

GEO ORBITS		MOLY ORBITS	
SATNO	27715	SATNO	7276
Ave (km)	2.3	Ave (km)	.8
Std Dev (km)	1.30	Std Dev (km)	1.06
SATNO	27954	SATNO	7800
Ave (km)	1.5	Ave (km)	1.0
Std Dev (km)	1.13	Std Dev (km)	0.70
SATNO	28252	SATNO	8015
Ave (km)	1.3	Ave (km)	0.5
Std Dev (km)	1.26	Std Dev (km)	0.36
SATNO	28790	SATNO	23587
Ave (km)	1.5	Ave (km)	1.8
Std Dev (km)	1.20	Std Dev (km)	1.30
SATNO	33275	SATNO	24764
Ave (km)	1.3	Ave (km)	1.4
Std Dev (km)	0.91	Std Dev (km)	1.42
SATNO	33453		
Ave (km)	1.8		
Std Dev (km)	1.23		

Table 2 shows the range residuals for a mechanical tracker at geosynchronous and Molniya orbits. The geosynchronous objects are the same as the objects in table 1 while the Molniya objects are random samplings. The range residuals were smaller than the triangulated ranges for geosynchronous cases and about the same for the Molniya cases. The standard deviation was smaller than a tenth of a kilometer for every case; therefore it is not included in the table.

Table 2: Mechanical Tracker Range Residuals

GEO ORBITS		MOLY ORBITS	
SATNO	27715	SATNO	37170
Ave(km)	0.2	Ave(km)	1.1
SATNO	27954	SATNO	33447
Ave(km)	0.5	Ave(km)	2.4
SATNO	28252	SATNO	25485
Ave(km)	0.9	Ave(km)	0.1
SATNO	28790	SATNO	29260
Ave(km)	1.4	Ave(km)	1.4
SATNO	33275	SATNO	29260
Ave(km)	0.3	Ave(km)	0.7
SATNO	33453	SATNO	28163
Ave(km)	0.6	Ave(km)	2.4

Figures 5 through 15 compare the error of the observations after differential correction when triangulated range is included versus an angles-only DC as shown in Method 2. Figures 5 through 10 are geosynchronous payloads, while Figures 11 through 15 are Molniya satellites. As mentioned in Method 2, the same data was used in the DC with the exception of the triangulated ranges.

Figure 5 and Figure 6 show the error growth of two geosynchronous orbits that have no range data other than triangulated range. They also have DC fit-spans that are too short due to maneuvers prior to the fit. Satellite 27954

shows a significant improvement in the error immediately while satellite 28252 shows improvement after two and a half days.

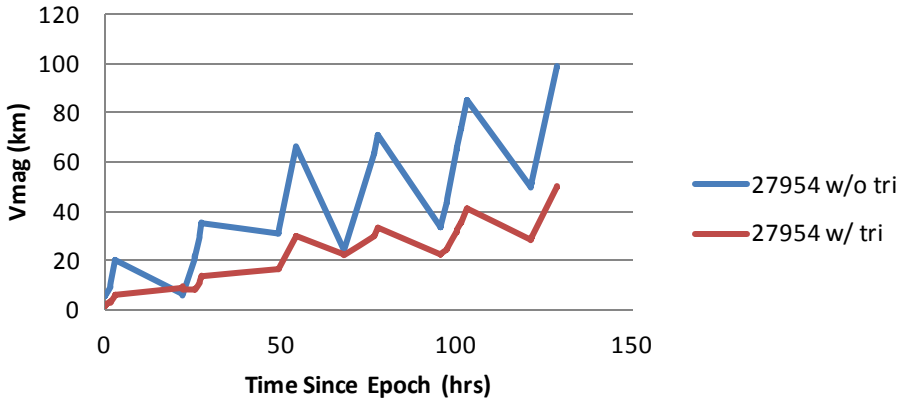

Figure 5: Error Growth of 27954

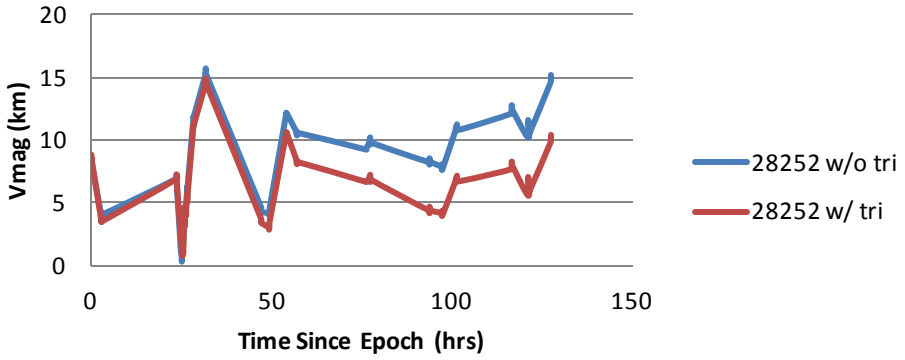

Figure 6: Error Growth of 28252

Figures 7 and 8 show the error growth of geosynchronous orbits that have mechanical tracker range observations included in the DC fit-span. There is no perceivable change in the error.

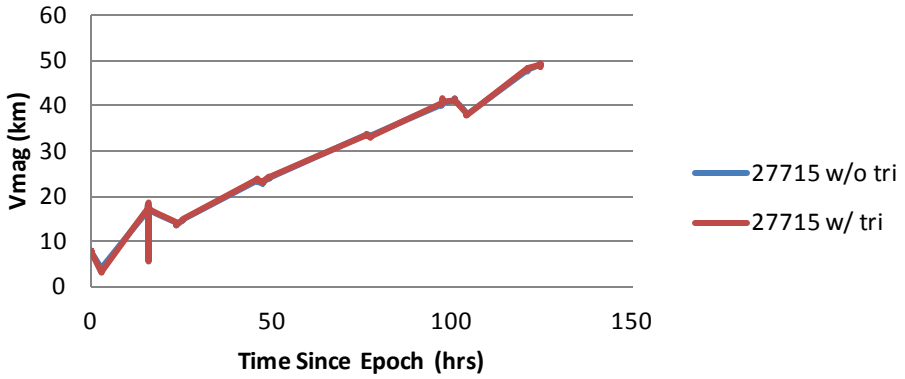

Figure 7: Error Growth of 27715

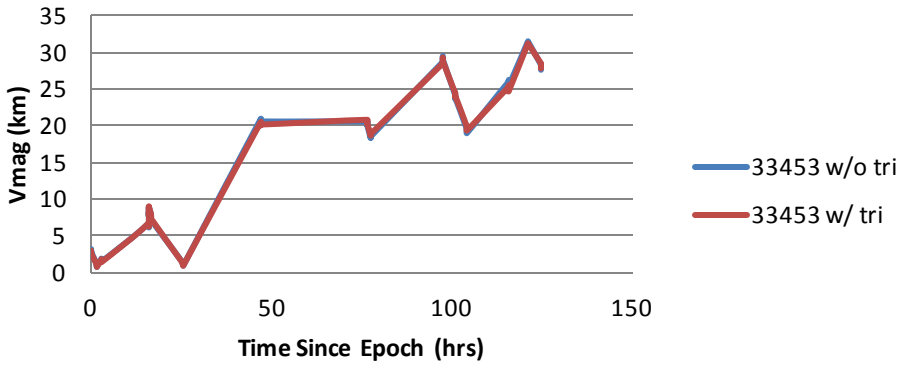

Figure 8: Error Growth of 33453

Figures 9 and 10 also show the error growth of geosynchronous orbits that have mechanical tracker range observations included. However, there is a station keeping maneuver shortly after the epoch for both satellites. The errors of both orbits started with small differences, but after the maneuvers the DCs with the triangulated range became more accurate.

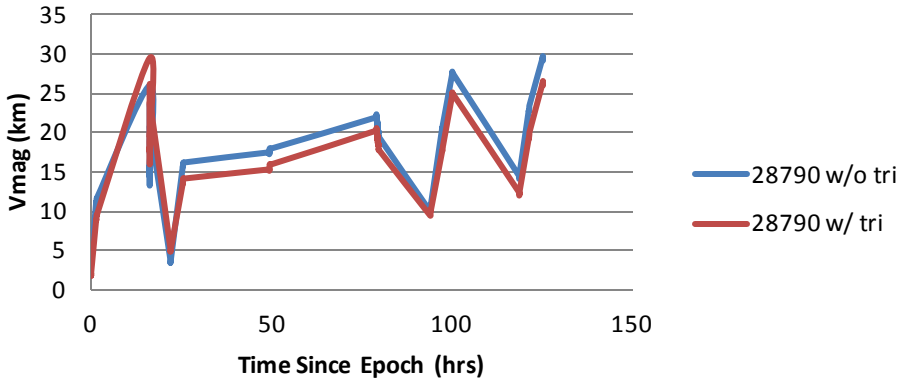

Figure 9: Error Growth of 28790

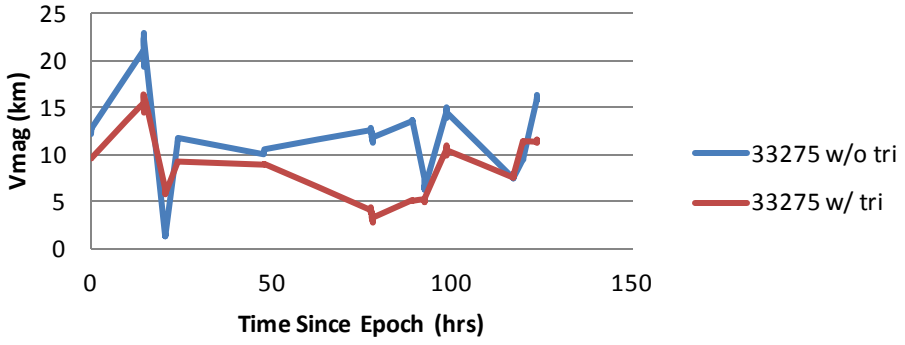

Figure 10: Error Growth of 33275

Figures 11 through 13 show the error growth of Molniya orbits with phased array range observations included. There is no significant difference when the triangulated ranges are included. In 7276, there is no difference in the error growth.

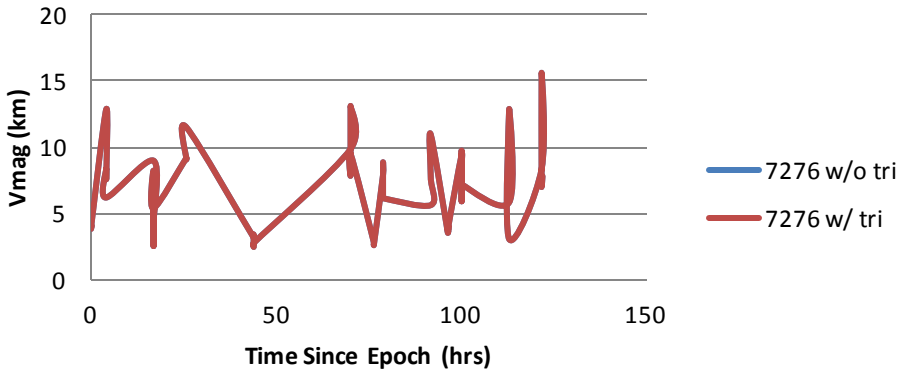

Figure 11: Error Growth of 7276

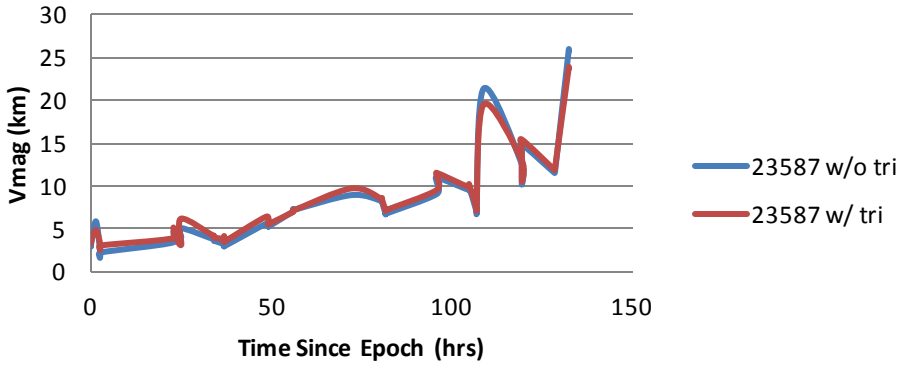

Figure 12: Error Growth of 23587

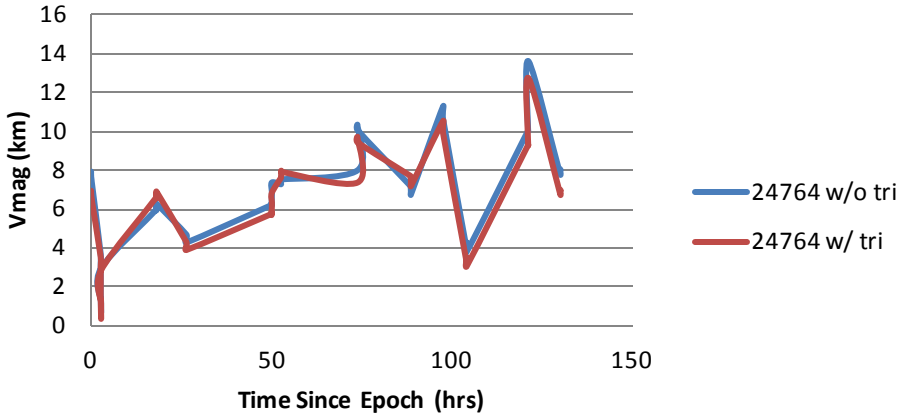

Figure 13: Error Growth of 24764

Figures 14 and 15 are Molniya orbits that have no range observations with the exception of triangulated range included in the DC. The difference in the error for satellite 7800 is a kilometer and 5 kilometers for satellite 8015. 8015 is more sparsely tracked than 7800; therefore, it has more to gain from using the triangulated range. In both cases, using triangulated range has made the differential correction more accurate.

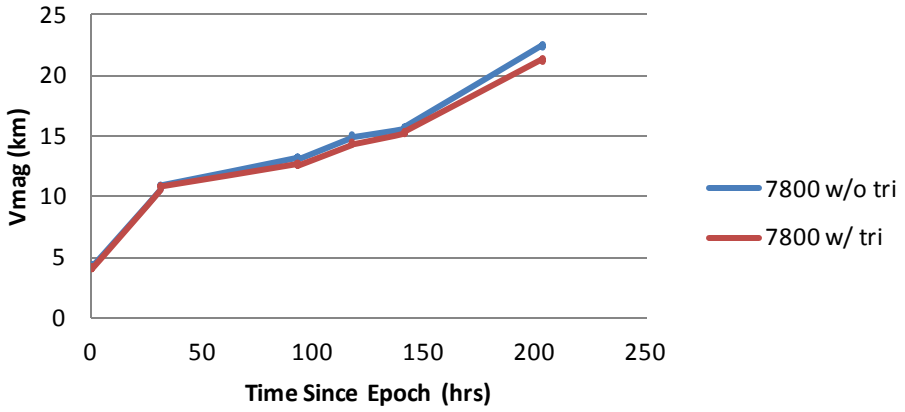

Figure 14: Error Growth of 7800

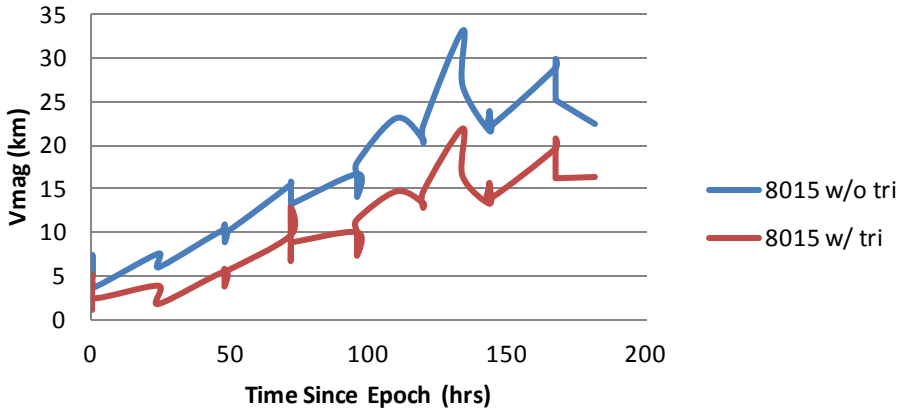

Figure 15: Error Growth of 8015

Figure 16 and Figure 17 show UCTs that were simultaneously tracked and processed by Method 3. The error of the next track was evaluated. In Figure 16, the error of the next track has decreased by forty to fifty kilometers by including the triangulated range. According to the ROTAS software, the cutoff between ASTAT 3 (poorly associated) and ASTAT 4 (unassociated) for this case is 300 kilometers of error. In Figure 16, the observations below the association cutoff line associated to the object while the observations above the object were unassociated. More of the track associated when the triangulated range was included.

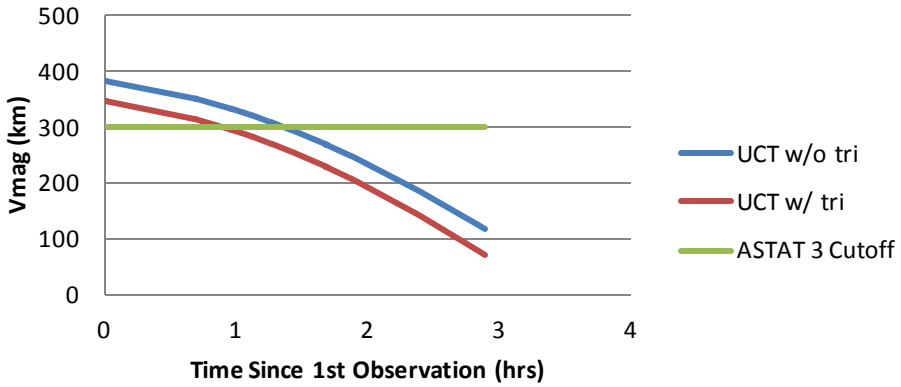

Figure 16: Error Growth of Triangulated UCT, 1 Day After Epoch

Figure 17 shows the error growth of the second UCT up to three days after epoch. Without the triangulated range, the error grows well above the ASTAT 2 cutoff shortly after the 24 hour mark. With the triangulated range, the error stays at ASTAT 0 until three days after epoch. If the object is tracked once a day, it will have three ASTAT 0 tracks over a three day period and can be maintained automatically by the system.

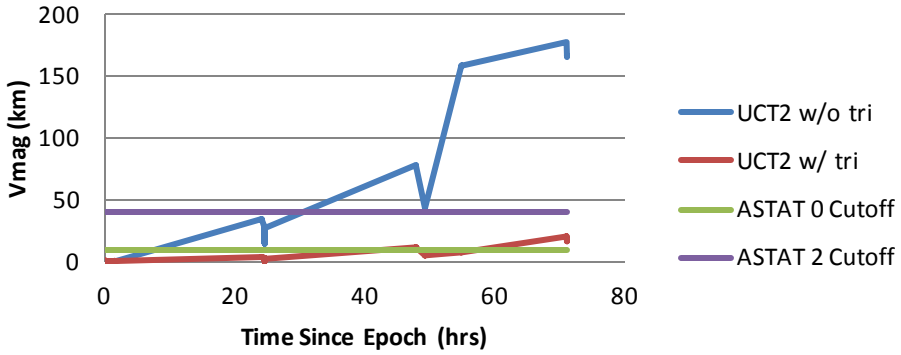

Figure 8: Error Growth of UCT2, Full Timespan

6. Conclusion

There is much to gain in the SGP4 theory by using triangulated range. The benefit will mostly be seen by geosynchronous orbits with DCs that have fit-spans that are too short, sparsely tracked objects, and in the area of GEODSS UCT processing. The ephemerides for sparsely tracked objects and objects with fit-spans that are too short will become more accurate because the DC will have real range data included. Analyst satellites created from GEODSS UCTs will be much easier to reacquire and will be able to be created from shorter tracks. To be included into the SP theory, a calibration has to be done for the triangulated range on a more extensive sample population. There must also be more test cases using the methods described above to get a more accurate assessment of the triangulated ranges and when to use them.

7. References

Sanders-Reed, John N. "Impact of Tracking System Knowledge on Multi-Sensor 3D Triangulation", SPIE 4714, April, 2002.